The Cryosphere Discuss., doi:10.5194/tc-2016-113, 2016
Manuscript under review for journal The Cryosphere
Published: 3 June 2016

The past, present, and future viscous heat dissipation available for Greenland subglacial conduit formation

Kenneth D. Mankoff[1] and Slawek M. Tulaczyk[2]

[1]Department of Geosciences, Pennsylvania State University, University Park, PA 16802
[2]Earth and Planetary Sciences Department, University of California Santa Cruz, Santa Cruz, CA 95064

Correspondence to: Ken Mankoff (mankoff@psu.edu)

Abstract.

Basal hydrology of the Greenland Ice Sheet (GIS) influences its dynamics and mass balance through basal lubrication and ice/bed de-coupling, or efficient water removal and ice/bed coupling. Variations in subglacial water pressure through the seasonal development of the subglacial hydrological system help control ice velocity. Larger conduits melted by the viscous dissipation of heat from surface runoff may lead to efficient drainage systems that lower subglacial water pressure, increase effective stress, and reduce ice velocity. Conduit opening occurs primarily due to viscous heat dissipation (VHD) associated with flow of subglacial water. In this study we quantify the energy available for VHD historically, at present, and under future climate scenarios. At present, 345 km^3 of annual runoff with a gravitational potential energy of 2.9 x10^{18} J (2.9 EJ) delivers 1.9 EJ to the base of the ice sheet per year. These values are already ~35% more than the historical 1900s average of 1.4 EJ year^{-1} at the bed which was comparable to geothermal heat flux (GHF) of 1.1 EJ year^{-1} under the runoff area. By 2100 under IPCC AR5 RCP8.5 (RCP4.5), 1278 (524) km^3 of runoff with gravitational potential energy of 14.3 (4.9) EJ year^{-1} will deliver 9.0 (3.2) EJ year^{-1}. In the future, there may be a ~5-fold increase in VHD, 100% of which is assumed to melt open subglacial conduits. In comparison, the area of the bed accessed by runoff remains roughly constant and therefore comparable GHF increases only slightly compared to historical values. With increasing surface meltwater penetration to the bed the basal heat budget in the ablation zone of the GIS will be increasingly dominated by VHD and relatively less sensitive to GHF, which may result in changes in the ice flow field and its seasonal variability.

1 Introduction

Numerical models and observations of the Greenland Ice Sheet (GIS) link surface meltwater penetration to the bed to both short (hourly, daily) and long (seasonal, decadal) temporal variations in ice velocity (Shannon et al., 2013; Zwally et al., 2002; Bartholomew et al., 2011; Banwell et al., 2013; Mayaud et al., 2014; Tedstone et al., 2015). However, the link between increased basal water inputs and ice sliding is a complex one, largely because viscous heat dissipation (VHD) from water flow beneath ice may melt out efficient drainage tunnels whose presence may decrease, or even reverse, the tendency for ice flow to accelerate with increasing meltwater inputs to the bed (Kamb, 1987; Sundal et al., 2011; Tedstone et al., 2015).

The Cryosphere Discuss., doi:10.5194/tc-2016-113, 2016
Manuscript under review for journal The Cryosphere
Published: 3 June 2016

Early in the melt season water is added to the subglacial system but cannot be efficiently removed, subglacial water pressures increase, and ice velocity increases. Later in the melt season, increased runoff causes efficient drainage conduits to form. These large drainage conduits reduce the subglacial water pressure and ice velocity (Hewitt, 2013). Even efficient drainage conduits can at times become over-pressured, with associated increase in ice velocity, until basal water is removed or the conduit opens more from additional melting (Schoof, 2010). The subglacial hydrologic system influences ice velocity during the non-melt winter months as well. This behavior is less well understood, but it appears that increased summer velocities may correlated to decreased winter velocities, with a total annual displacement that is less than in years without the larger summer speed-up (Sundal et al., 2011), and a recent observational study shows a regional and decadal velocity decrease coincident with a 50% runoff increase in southwest Greenland (Tedstone et al., 2015).

The majority of studies examining surface melt, supra-glacial routing, subglacial hydrology, and the response of ice sheet outlet glaciers to those various inputs takes place in southwest Greenland, often near the Russell and/or Leverett Glaciers (for example, Banwell et al. (2013); Arnold et al. (2014); Andrews et al. (2014); Tedstone et al. (2015)). Furthermore, present day weather, runoff, outflow, and other data is often used in those studies, since daily, hourly, or higher temporal resolution of the data is beneficial to the models. However, using present data limits their focus to some recent seasons for which abundant in-situ sensor data exists. In order to examine future scenarios, Mayaud et al. (2014) built on the work of Banwell et al. (2013), but used a conduit model that includes melt opening and creep closure, driven by a positive degree day runoff model, to examine future changes to year 2095 under various IPCC RCP scenarios (Moss et al., 2010). Those models had hourly or daily resolution and were again limited to the well-studied ~200 km^2 area near Russell glacier.

Here we perform a broader analysis that examines runoff over the entire GIS on annual and decade timescales, and frame the discussion in terms of changes in heat available to melt open conduits (VHD), rather than focusing on water pressure in a conduit relative to overhead ice pressure. We report both the total GIS-wide energy budgets, its distribution at a 5x5 km grid resolution, and highlight results along one flowline at 150 m resolution. We examine what fraction of the initial gravitational potential energy of surface meltwater converts to heat subglacially and is used for subglacial melting. Our treatment of en- and sub- glacial hydrology is simplified because it does not represent actual conduits, but is at the same time more comprehensive than in existing global climate or ice-sheet models (e.g. Pollard and DeConto (2012)), and may offer a computationally efficient yet improved method to incorporate glacial hydrology at their existing grid resolution.

2 Data

We use a 150 m resolution basal topography and surface topography (IceBridge BedMachine Greenland, Version 2) from Morlighem et al. (2014, 2015) to calculate both surface and subglacial flow routing and subglacial pressures. Surface runoff, equal to the surface meltwater and rain that does not re-freeze but instead runs off, comes from MARv3.5.2 (Fettweis et al., 2013).

We report results for a historical period (1900 – 1999), the present (2010 – 2019), and IPCC AR5 RCPs 4.5, and 8.5 (2090 – 2099) (Moss et al., 2010). We process the entire GIS at 5 km resolution, and then part of West Greenland (near the Russell and Leverett glaciers) at 150 m resolution, where we extract a flowline segment.

3 Methods and assumptions

We introduce our methods and assumptions by tracing the path of a unit parcel of surface meltwater from source to sink (ice surface elevation at the origin of a meltwater parcel to sea or land-outlet level where it discharges from an ice sheet). We follow a simplified form of Bernoulli's equation,

$$\frac{p_s}{\gamma} + z_s + \frac{v_s^2}{2g} = \frac{p_b}{\gamma} + z_b + \frac{v_b^2}{2g} + H_L, \tag{1}$$

with p pressure, γ the specific weight of water, z elevation above sea level, v velocity, g gravitational acceleration, and H_L combined head loss (e.g. Gulley et al. (2014)). Subscripts s represent the ice surface and b, the bed. Viscous heat dissipation (VHD) is the process that causes head losses H_L. Eq. 1 is in units m and the three terms are often referred to as the pressure head, elevation head, and velocity head. It can be multiplied by mg and then it is an energy balance equation, with the middle term the gravitational potential energy.

We describe the model used to route surface runoff to the bed and down the hydropotential gradient, where subglacial conduits melt open from VHD in flowing water (Fig. 1). At each step we detail the assumptions made, the amount of energy available to the parcel of water with respect to the initial gravitational potential energy, and the form of that energy: gravitational potential, kinetic (velocity), pressure, or transferred out of the water parcel as sensible heat.

3.1 Surface runoff and routing

Surface runoff comes from melted ice or rainfall that does not refreeze or evaporate. At its source it has a total gravitational potential energy, PE_{total},

$$PE_{\text{total}} = mgz_s. \tag{2}$$

Results of Eq. (2) are shown in Fig. 2. We assume that initially water has only its gravitational potential energy available and has negligible velocity and kinetic energy and it is initially at 0 °C at atmospheric pressure.

Runoff with an initial elevation > 2000 m has low liklihood of penetrating to the bed (Poinar et al., 2015), and is instead routed on the surface to below 2000 m elevation. Elsewhere, runoff may leave the surface within its source grid cell. Side-draining lakes and supraglacial streams transport horizontally by definition, and moulins often drain these to the bed near their source (Yang and Smith, 2013). Surface meltwater may on average flow 5 – 10 km (1 – 2 grid cells in our model) before leaving the surface (Yang et al., 2015). However, we ignore this horizontal transport because when streams do travel this far on the surface, they are most likely to do so in crevasse-free regions of ice sheets that are subjected to relatively low strain rates and stresses (Poinar et al., 2015) implying a flatter surface. Horizontal transport of surface meltwater with a small elevation drop has only a small impact on the initial gravitational potential energy. Horizontal transport in an area with large surface slope and impact on gravitational potential energy is unlikely, because such regions have high driving stress, and crevasses routing the stream to the bed are likely to be present.

Near-surface water storage may occur, but because we discuss results on an annual and longer timescale and focus on change over time, only changing relative amounts of storage would affect the results, and only in amounts larger than a few percent of the total runoff volume. Near surface water storage and refreezing are not addressed here but the surface mass balance model that generates the runoff takes some refreezing into account (Fettweis et al., 2013).

3.2 Transit from the surface to the bed

We assume all water reaches the bed within the 5x5 km grid cell where it leaves the surface. Moulins and crevasses, either at a lake bottom or when a supraglacial stream leaves the surface, carry water from the surface to the bed. Although the exact path to the bed is poorly constrained, moulins generally deliver their water to the bed within a few ice thicknesses (Gulley, 2009).

When falling through the air-filled portion of a moulin or crevasse, part of the initial gravitational potential is converted to kinetic energy and then dissipated as heat to the surrounding air, moulin and crevasse walls, and water table surface on impact.

We assume the density of ice is 917 kg m^{-3}, the density of water is 1000 kg m^{-3}, and that the subglacial system is pressurized to slightly less than the ice-overburden pressure as often observed in the field (Engelhardt and Kamb (1997); Fountain (1994); Meierbachtol et al. (2013)). Given the above, the water table in the moulin will be ~90% of the way up the moulin when the subglacial system is near the ice-overburden pressure. In this case, stationary water at the surface of a 90% water-filled moulin retains ~90% of its initial gravitational potential energy and dissipated ~10% to heat (Fig. 1), which we consider "lost" from the system. The potential energy available at the moulin water table surface relative to the terminus elevation is therefore a subset of PE_{total} (Eq. 2), equal to,

$$PE_{\mathrm{moulin}} = 0.9\, m\, g\, (z_s - z_b) + m\, g\, (z_b - z_o), \tag{3}$$

with z_o the elevation of the outflow at the terminus. Moulins do not conduct significant heat to ice (Lüthi et al., 2015), and while we assume all potential energy is converted to pressure energy along the descent, we also assume that water remains at the phase transition temperature (PTT),

$$PTT = C_T\, (z_s - z_b)\, \rho_i\, g \tag{4}$$

derived from C_T the Clausius-Clapeyron slope equal to 8.6x10^{-8} K Pa^{-1} (Hooke, 2005), and ρ_i the density of ice. Water captured by crevasses also warms ice as it refreezes (Phillips et al., 2013). We do not consider either of these processes that release heat englacially because they do not occur at the bed, and the crevasse-captured water volume is negligible relative to the total surface runoff volume.

The Cryosphere Discuss., doi:10.5194/tc-2016-113, 2016
Manuscript under review for journal The Cryosphere
Published: 3 June 2016

In our model, the PTT adjusts the total energy by ~30% and is not zero sum even though input and output are both at atmospheric pressure (PTT = 0 °C). From the specific heat of water (c_p = 4190 J kg^{-1} K^{-1}), and the equation $(g\,z)/c_p$, water can warm 0.0023 °C per m of elevation drop. A unit mass of water at z_s = 1000 m has gravitational potential energy of ~10000 J and can therefore warm itself by 2.3 °C if lowered to 0 m. From Eq. 4, the Clausius-Clapeyron slope reduces the PTT -0.7 °C due to the pressure under 1000 m of ice, equal to ~1/3 of the temperature change from gravitational potential energy. However, as stated previously we do not consider this initial change in PTT in the moulin because that occurs englacially. As the water flows out and returns to atmospheric pressure (for land-terminating glaciers), we do consider changes in the PTT, meaning ~1/3 of the potential energy may used internally by the water to increase its temperature with the PTT as the PTT returns to 0 °C (Röthlisberger, 1972).

3.3 Flow routing at the bed

Once at the bed, water is routed from one grid cell to the next based on the gradient of the hydropotential ϕ calculated from the ice surface and bed elevation, and decomposed into elevation potential ϕ_z, and pressure potential ϕ_p,

$$\phi = \phi_z + \phi_p = \rho_w\,g\,z_b + \rho_i\,g\,(z_s - z_b), \tag{5}$$

with ϕ, ϕ_z, and ϕ_p in units Pa. ϕ equals the potential energy per unit volume of water, and dividing by $\rho_w\,g$ gives the hydraulic head (Cuffey and Paterson, 2010). All water is assumed to move to the neighboring cell (of 8) with the lowest hydropotential and conduits are not included in the model. This flow routing redistributes the surface source into subglacial streams (Fig. 3). Flow routing is implemented using the `r.watershed` tool in grass GIS (Neteler et al., 2012) version 7.0.3, with ϕ as the "elevation" input with all "sinks" filled so that all water leaves the ice sheet (see Supplemental Material).

The change in hydropotential that drives flow comes from a combination of Eq. (5) and the downstream cell from the flow routing algorithm, or,

$$\Delta\phi = \phi_i - \phi_{i+1}, \tag{6}$$

where water flows from grid cell i to cell $i+1$. $\Delta\phi_z$ and $\Delta\phi_p$ are defined similarly to Eq. (6).

The net hydropotential change $\Delta\phi$, does not distinguish between flow driven by changes in basal elevation which does not change the PTT, and flow driven by changes in ice thickness or pressure which does change the PTT. Our decomposition of $\Delta\phi$ into $\Delta\phi_z$ and $\Delta\phi_p$ (Eq. 5 and 6, Fig. 4) allows us to estimate where potential energy losses occur due to an elevation drop and where potential energy losses occur due to a pressure drop. This distinction matters because if flow is driven by an elevation drop (red $\Delta\phi_z$ in Fig. 4), ice thickness may increase, decrease, or remain constant, and those three scenario imply a $\pm 2/3$ change in the heat released due to the pressure change. Similarly, if flow is driven by a pressure drop (red $\Delta\phi_p$ in Fig. 4), ice must thin along-flow, and ~1/3 of the potential heating from the pressure drop is not released (Röthlisberger, 1972). These ~1/3 and ~2/3 values come from the PTT, the specific heat of water, and the density of water, or $C_T\,c_p\,\rho\ \approx 1/3$.

3.4 Basal viscous heat dissipation

As water flows down the hydropotential gradient, we track the energy released as heat (Q) based on the volume of water, the change in the hydropotential, and the change in the PTT,

$$Q = V(\Delta\phi - C_T\, c_p\, \Delta\phi_p\, \rho_w) \tag{7}$$

where V is the volume of water (Fig. 3), $\Delta\phi$ is the net hydropotential change along flow from cell i into $i+1$, and $\Delta\phi_p$ is the pressure component of the hydropotential change along flow. The last term of Eq. (7) is an adjustment for the PTT, which increases the heat released along the flowline when the ice thickens down-stream ($\Delta\phi_p$ is negative, and the PTT drops), and reduces the heat released along the flowline when the ice thins downstream. If second term on the RHS of Eq. 7 is larger than the first term on the RHS, then Q is negative, and basal freeze-on occurs (Alley et al., 1998; Bell et al., 2014)

3.5 Energy advected from the system as sensible heat or velocity

In an idealized scenario where water exits a glacier at sea level, it will have lost 10% of its initial gravitational potential energy at the beginning of its journey through the air-filled portion of the moulin and dissipated the remaining 90% as heat during its flow through the englacial and subglacial drainage system. In reality, most water leaves glaciers above or below sea level. When water leaves the ice sheet margin from a land-terminating glacier all water pressure in excess of atmospheric pressure is released and only gravitational potential energy corresponding to the elevation of the glacial outlet above sea level remains (Fig. 1).

Only a small fraction of the total gravitational energy drop is converted to kinetic energy (velocity) (Liestøl, 1956). This can be illustrated by the fact that a 1 kg unit parcel of water has gravitational potential energy of ~10000 J when it is at 1000 m elevation, and kinetic energy of ~50 J (only 0.5% of the initial gravitational potential energy) if it flows out of the terminus at a relatively fast velocity of 10 m s^{-1}. Given that meltwater is at atmospheric pressure and in contact with ice between the entrance (e.g., moulin) and exit (e.g., ice-marginal tunnel) there should be no significant net change in water temperature and no significant change in heat content between the input and output ends of the hydrological system. Hence, the bulk of the gravitational energy loss experienced by surface meltwater will be dissipated as heat during subglacial water flow. Early work in glacier hydrology indicate that this heat is used to melt ice in contact with the flowing water (Shreve, 1972; Röthlisberger, 1972). When water leaves an ice margin under a marine-terminating glacier, the same processes occur releasing heat subglacially, but the water at the exit point does not return to atmospheric pressure but rather to the pressure determined by the depth below sea level at which subglacial outflow takes place (Fig. 1).

Water also does not leave the system with significant energy in the form of sensible heat. Two separate arguments support this proposition, in addition to the bulk of existing subglacial fluid thermal transfer literature: 1) laboratory experiments, and 2) measurements in proglacial streams.

The standard assumption in the subglacial hydrology literature is instantaneous heat transfer (Röthlisberger, 1972; Clarke, 2003; Hewitt, 2011), combined with all heat being delivered to the ice or used to maintain the water at the phase-change temperature (Catania and Neumann, 2010; Röthlisberger, 1972; Clarke, 2003; Hewitt, 2011; Fountain and Walder, 1998), with only the following few exceptions: Mathews (1973) examined subglacial outflow from an active volcanic/geothermal terrain where water may be starting with temperatures far above the freezing point. Hock and Hooke (1993), when re-analysed with the correct heat capacity of water (pers. comm.; the heat capacity of water is not 256.9 J kg^{-1} K^{-1} as in Hooke (2005)) report that 15% is advected. Röthlisberger (1972) assumes instantaneous heat transfer for the bulk of that paper, but on page 197 suggests 10 - 50% of energy may leave a subglacial system unused. However, his citation is personal communication with Mathews (in press), cited as "Mathews, W. H. In press. Record of two jökullhlaups (1969)". We find no such paper, but Mathews (1973) has an identical title and reports through one method that only 20-50% of energy is used to melt ice (50-80% leaves the system as sensible heat), and through another that 10 - 50% is lost to advection (as quoted by Röthlisberger). A manuscript written by Rist (1954) in Icelandic is interpreted (translated) by two different sources. Nye (1976) reports 0.05 °C (water can be warmed 0.05 °C by lowering it 21 m) but approximates that as 0 °C, and Björnsson (2010) reports that Rist (1954) has repeatedly measured outflow at 0 °C. We are aware of no other manuscripts suggesting that sensible heat is advected from the subglacial environment with discharging water and the few examples to the contrary come from either glacial systems in Icelandic volcanic terrain (e.g. Mathews (1973)) or a glacier with a very short drainage pathway (Hock and Hooke, 1993).

Laboratory experiments indicate that water flowing through ice reaches a near-zero equilibrium temperature within 10s to 100s of m (Isenko et al., 2005). An independent method measuring and modeling proglacial stream temperature closes the heat budget with an outflow of 0 °C, with stream temperatures above that attributed to one of four sources occurring between the glacier snout and thermometer: net shortwave radiation, evaporative heat flux, sensible heat flux, and streambed friction (Chikita et al., 2010). The lab and pro-glacial stream experiments do not address temperature changes due to the pressure-dependence of the phase change of water.

Even if all heat is consumed under the glacier, the assumption that all heat is transferred to the ice is likely violated as some energy may be used for eroding and/or transporting debris, fracturing ice, generating seismic waves, and to heat subglacial materials (Tsai and Rice, 2010; Evans et al., 1998). We assume that these terms are negligible, and note that some of these, like heating of subglacial materials, are likely to be intermediate processes that themselves will re-release heat. We therefore neglect these terms, assuming as much of the existing subglacial hydrological heat transfer literature does that melting of basal ice represents the ultimate sink of heat beneath wet-based ice masses. Due to background geothermal flux, subglacial geologic materials will normally be warmer than ice and, by the second law of thermodynamics, heat will flow from the warmer subglacial material towards colder ice.

We treat the energy used to transport bedload as net zero within each model grid cell. Because the energy used to pick up bedload is returned when the bedload drops, only bedload transported across the terminus impacts the total energy available for heating. Large volumes of fine sediment are carried across the terminus boundary, but the kinetic energy of that sediment is a small fraction of the kinetic energy of the water (which was previously shown to be negligible), and we therefore do not consider it.

3.6 Methods and assumptions summary

We conjecture that nearly all the gravitational energy loss experienced by surface meltwater as it travels through and beneath the Greenland ice sheet is ultimately used to melt ice in contact with englacial and subglacial water drainage pathways. Our model closes the energy budget by assuming that 90% of the potential energy loss experienced by surface meltwater is simply balanced by heating and melting under the ice sheet in the ideal scenario of a flat bed and outflow at sea level. This is equivalent to stating that all terms on the RHS of Eq. 1 approach 0 at the outflow, except for H_L, which must balance the high elevation term on the LHS. If some fraction of the gravitational energy loss of water flowing under ice sheet is converted into some other form of energy neglected here, it is worth noting that the central focus of this paper is on examining changes over time, and the impact of the neglected terms is muted as long as they do not change relative magnitude over time.

4 Results

4.1 Gravitational potential energy

The source term, gravitational potential energy of surface runoff, is shown in Fig. 2 in units of both energy and as annually averaged energy flux rate (i.e. power). Energy measured in Joules comes from the runoff volume multiplied by density to get mass, and power in Watts comes from dividing the energy by the number of seconds in a year. Summing across the ice sheet (Fig. 2) gives annual GIS-wide gravitational potential energy of 2.1, 2.9, 4.9, and 14.3 times 10^{18} J (or exajoules, EJ) year^{-1} for the historical, present, RCP4.5 and RCP8.5 cases respectively after the surface runoff is routed to the 2000 m contour (Table 1). The same result can be found by evaluating Eq. (2) with total annual runoff volume of 345 km^3 times 1000 kg m^{-1} and the volume-weighted mean elevation of 863 m for the present day case (Table 1).

4.2 Viscous heat dissipation

A spatial map of basal VHD is shown in Fig. 5 with the energy calculated based on Eq. (7). Summing the spatial data in Fig. 5 gives annual GIS-wide VHD of 1.4, 1.9, 3.2, and 9.0 EJ year^{-1} for the historical, present, RCP4.5 and RCP8.5 cases respectively (Table 1). These numbers are ~65% of the incoming gravitational potential energy respectively, which is below the theoretical value of ~90% discussed above. The difference is due to initial bed topography below sea level, land terminating glaciers discharging above sea level, and the pressure dependence of the phase transition temperature. For example, if a parcel of water begins at 1000 m elevation over a -1000 m bed and discharges at 100 m elevation (Fig. 1), the following processes reduce VHD: 1) the 90% of ice overburden basal pressure means that the moulin water level is at 1800 m above the bed (800 m above sea level), and 20% instead of 10% of the initial gravitational energy relative to sea level is dissipated before surface meltwater reaches the water table (Eq. 3), 2) water discharges at 100 m elevation rather than at sea level, so the total potential energy drop through the englacial and subglacial drainage system is due to 700 m of elevation change (Eq. 3), and 3) the impact of the PTT should be net 0 from inflow to outflow because both are at atmospheric pressure, but is not net 0 because due to the instantaneous heat transfer assumption, and the fact that our model only tracks VHD at the bed (Eq. 4). Water that enters the

The Cryosphere Discuss., doi:10.5194/tc-2016-113, 2016
Manuscript under review for journal The Cryosphere
Published: 3 June 2016

model at the moulin bottom is at the PTT below 0 °C, and energy is consumed warming it as the ice thins (Eq. 7). Beyond this specific example, if outflow occurs at marine terminating glaciers under thicker ice than where the water entered the system, that water has the ability to release excess heat due to the PTT.

Frictional basal heating is up to 0.2 W m^{-2} near the Russell and Leverett glaciers (Brinkerhoff et al., 2011), while geothermal heat flux (GHF) is estimate at ~0.050 W m^{-2} (Shapiro and Ritzwoller, 2004) to as little as 0.030 W m^{-2} (Meierbachtol et al., 2015). The logarithmic scale used in Fig. 6c makes the differences between these heat sources and VHD appear small, but near the margin VHD exceeds the expected values of GHF by one to two orders of magnitude. At present, VHD releases more heat than GHF from ~50 km inland to the margin. In the future, when larger volumes of water flow from farther in the interior, the zone where VHD surpasses GHF may increase its reach to ~100 km upstream from the ice margin (Fig. 6c).

5 Discussion

5.1 Conduits v. distributed flow

The routing model and energy balance model above are based on the hydropotential which we derive using only ice sheet surface and bed geometry, and the common assumption that subglacial water pressure is equal to ice overburden pressure everywhere. The latter represents a reasonable approximation for distributed subglacial drainage systems (e.g. Engelhardt and Kamb (1997); Fountain (1994); Meierbachtol et al. (2013)). There are no conduits in this model, although it is likely that conduits would form along the paths where maximum flow and heating occurs (Fig. 3 and 5). Conduits are unlikely to form deep in the interior (Dow et al., 2014) and in the well-studied Russell/Leverett region have been observed up to 34 km inland (Meierbachtol et al., 2013). When conduits do form, they should draw down local subglacial water pressures, which will result in increased VHD wherever pressurized subglacial water drains from the distributed drainage system into the lower-pressure conduit system. Since the current model does not explicitly represent pressure drops into conduits, this will occur farther inland than represented here. Our model may therefore be overstating the concentration of VHD near the ice sheet margin and development of conduits will spread the heat dissipation more evenly over areas further inland.

5.2 Heat at the ice sheet bed

Flow routing and VHD are similar, but not the same. Basal water is routed based on the change of the net hydropotential (Eq. 6, Fig. 4). Viscous heat dissipation (Eq. 7, Fig. 5) is similar to V times Eq. (6), but Eq. (7) has a second term on the RHS, which states that 1/3 of the heat that could be released due to thinning ice remains in the water, raising its temperature along with the PTT. For certain elevation changes Q is negative and basal freeze-on may occur (blue pixels in Fig. 5). Locations of basal freeze-on in the model may be due to the physical processes described above, or due to the basal DEM not actually representing the basal topography and flow paths. Where basal re-freezing occurs, additional heat is released and new warm ice is generated (Alley et al., 1998; Bell et al., 2014). Predicted locations of basal freezing are near where Bell et al. (2014) shows basal freeze-on packages, but do not exactly line up, suggesting there may be an error in either this model, the basal topography from Morlighem et al. (2014) input to the model, or that some advection occurred between results here and results in Bell et al. (2014).

Because the heating term is a function of water flux rate, it is spatially heterogeneous at the glacier bed. Flow routing creates subglacial conduits systems that accumulate several orders of magnitude more water than the surrounding non-conduit region (Fig. 3) and along a flowline water flux will increase (Fig. 6b). Variations in bed topography and ice thickness create variations in the rate of change of ϕ along the flowline (Fig. 6a), which leads to heterogeneous heating, and variations in melting rate along the flowline (Fig. 6c). At present when using a 5 km grid, the cell with the maximum discharge experiences a flux of 7 km^3 year^{-1} (2% of the annual runoff from the entire ice sheet). That percentage remains roughly unchanged, and by the end of this century under RCP8.5, one subglacial conduit may discharge up to 32 km^3 year^{-1} (Fig. 3). These large water fluxes focused into parts of the model domain mean that up to 10 W m^{-2} can be dissipated in such locations (Fig. 5 and 6c).

We assume that all the heat released from the water is used to melt ice and most of that to form subglacial conduits, and that most conduits form due to VHD from surface runoff because runoff-sourced water dominates basally-produced water, and as shown here VHD dominates GHF. This new basal-source meltwater leaves the ice sheet as latent heat (Fig. 1). This additional melt represents a small fraction of the total runoff - it is approximately 2%, or 7 km^3 year^{-1} at present and 32 km^3 year^{-1} under RCP 8.5 near year 2100. Although small by percent, the total volumetric increase is important when one considers that the bulk of subglacial conduit formation is represented by that 7 (present) or 32 (future) km^3 year^{-1}.

Regardless of the partitioning of the energy between melt and other processes not addressed here, the relative percentages will likely remain near their present value. Therefore, ~5 times the amount of energy is available for subglacial conduit formation under RCP 8.5 in year 2100.

Some future additional heat will be distributed over a longer fraction of a year relative to the present since climate warming prolongs the melt season in Greenland (Hanna et al., 2008). It will also be distributed spatially further inland relative to the present as the subglacial conduit network expands inland. When VHD occurs in new locations at the GIS bed it may convert a frozen bed to temperate and increase ice sliding (Parizek and Alley, 2004; Shannon et al., 2013). However, even if some future additional VHD reaches new locations inland and new times of the year due to an increased melt season, the bulk of it will occur in the same place, but it will have higher magnitude. The long-term effects of increased basal water on ice velocity are uncertain, but it appears that short-term velocity increases (Iken and Bindschadler, 1986), especially due to variable input (Schoof, 2010), may lead to overall summer acceleration but annual deceleration (Sundal et al., 2011), and decadal slowdown (Tedstone et al., 2015). At marine terminating glaciers, the process ought to be similar, but the effect is likely to be less important than other processes determining glacier velocity and its variability (e.g. Walter et al. (2012)).

The integrated change in heat per flowline in shown in Fig. 7, with a minimum cutoff removing all small increases. The change between historical and present (P-H in Fig. 7) shows that at present, most of the increase is found in the sector where Tedstone et al. (2015) suggests a 50% increase in runoff has led to a reduction in glacier velocity. Up to 1.8x10^8 J more heat is released along one flowline, and a similar amount in several nearby flowlines, in this region. That amount may double under RCP 4.5, and increase by an order of magnitude under RCP 8.5. If the correlation between runoff and velocity is controlled by an increase in basal conduit size, quantity, or duration due to VHD, then in the future under RCP 8.5, a widespread reduction in glacier velocity may occur.

5.2.1 Geothermal Heat Flux

GHF is spatially and temporally more uniform than VHD which is concentrated in subglacial conduits and primarily occurs when surface melt is active. Nonetheless, it is worth comparing the magnitude and distribution of the two. Historically the total VHD of 1.4 EJ year^{-1} under the runoff area was similar to the total GHF of 1.1 EJ year^{-1} in that same area. That is no longer the case, and by the end of this century under RCP 8.5, VHD will contribute ~9 EJ year^{-1} while GHF only increases to 1.4 EJ year^{-1} due to a slight increase in the runoff area that reaches the bed (when surface runoff is routed to 2000 m elevation before moving to the bed).

VHD dominates other basal heating terms considered in some glaciological models (for example, Brinkerhoff et al. (2011)). Small differences in GHF estimates produce drastically different GIS growth scenarios (Rogozhina et al., 2012), and observed basal temperature measurements do not always agree with assumptions used in existing models (Meierbachtol et al., 2015). Increased geothermal heat flux also coincides with onset of fast ice flow (Fahnestock et al., 2001). The results of our analysis and these GHF studies suggest that if VHD contributes ~6 times as much heat in the future as historically, it may generally decrease the importance of GHF in modulating spatial dynamics of the ice sheet because it will swamp the basal supply of heat from GHF, at least underneath the ablation zone.

5.3 Erosion and sediment transport

Large amounts of eroded material are also flushed out from under the GIS each year (Cowton et al., 2012). The erosion rates implied by the sediment flux is already several orders of magnitude above the background (>1000 year) erosion rates (Koppes and Marchant, 2009). If 5 times the amount of water flows along the GIS bed by the end of the century, it may increase sediment removal (Bogen and Bønsnes, 2003). If increased VHD and water at the bed of the GIS simultaneously causes sediment removal rates to increase 5-fold for ~100 – 1000 years, while at the same time reducing the glacier velocity (Tedstone et al., 2015) and therefore the production of sediment (Herman et al., 2015), the state of the bed may rapidly change over the coming century from potentially deformable subglacial sediments to rigid bedrock (Weertman, 1964; Kamb, 1970; Tulaczyk et al., 2000; Bougamont et al., 2014)

5.4 Model domain

The model domain has 5x5 km grid for most of the analysis presented here, which means results are smoothed over that area. In reality, subglacial discharges occur on the order of one every 5 km along the coast (Lewis and Smith, 2009). For example, a discharge of 1000 m^3 m^{-2} year^{-1} of water in a 25 km^2 grid cell in Fig. 3(8.5) equals 25 km^3. That same 25 km^3 might discharge through a conduit on order 10 – 100 m wide, rather than the 5000 m wide cell used in the analysis. If a single conduit on the order of 10 – 100 m wide carries all of the water (Fig. 3) and is subject to all of the heating (Fig. 5), then values reported

The Cryosphere Discuss., doi:10.5194/tc-2016-113, 2016
Manuscript under review for journal The Cryosphere
Published: 3 June 2016

(here spread over 5000 m) are likely be one or more orders of magnitude larger in small focused regions, and one or more magnitudes smaller outside the conduit.

6 Conclusions

Large volumes of supraglacial runoff observed in Greenland ablation zone, including at relatively high elevations above sea level, contain large amounts of gravitational potential energy. We estimate that approximately 65% of this energy is dissipated as heat at the ice sheet bed in the ablation zone. This energy averaged 1.4 EJ year^{-1} over the 1900s, but has recently increased to 1.9 EJ year^{-1} and will likely increase to 3.2 or 9.0 EJ year^{-1} by the end of the century under RCP 4.5 or 8.5 respectively. Viscous heat dissipation will become the dominant basal heat source, and under RCP 8.5 will swamp the ~1 EJ year^{-1} contributed by geothermal heat flux in the same area.

This up to 6 times additional future heat at the ice sheet bed (relative to the historical amount) should result in a similar 6 fold increase in basal ice melt volume and may contribute to more, larger, longer-lasting, and more widespread subglacial conduits. The effect of increased conduit formation is not captured by this model, but based on recent results and subglacial theory, may decrease glacier velocity. This decrease may be offset by other processes and there may still be a net acceleration, especially at marine terminating glaciers. Along with possible impacts on ice velocity due to changing subglacial conduit configuration, increased runoff will remove more sediments, which will likely change the stress state at the glacier bed by changing the glacier/till/bedrock interface.

Appendix A: About This Document

This is an attempt to create a "fully reproducible" scientific publication. We may not have succeeded, but have made progress in this direction. In order to be fully reproducible at the binary-level, a clone of our operating system with the full analysis software should be provided. This could be done with a virtual machine (VM) but we have not taken this step because VMs require ~20 GB of space, and journals do not yet support this type of supplemental material.

Instead, we used only free and open source software above the operating system level, document in detail the version(s) of all software packages used, and provide every line of code required to reproduce the document, beginning with the commands to download the MAR (Fettweis et al., 2013) and IceBridge BedMachine Greenland, Version 2 (Morlighem et al., 2015, 2014) data sets, followed by the grass GIS (Neteler et al., 2012) and Python commands to produce intermediary data products and graphics.

The supplementary data is a plain-text file that contains the manuscript text and all of the code. As plain text, it can be viewed in any editor or document viewer. However, it's internal structure is that of an Emacs Org Mode (Schulte and Davison, 2011; Schulte et al., 2012) file and is best viewed in Emacs, which supports execution of the embedded code blocks. A reader should be able to reproduce the contents of this document, although it will require 3rd-party applications (GRASS, Python, etc.), and a similar system-level Emacs configuration as the authors.

The Cryosphere Discuss., doi:10.5194/tc-2016-113, 2016
Manuscript under review for journal The Cryosphere
Published: 3 June 2016

Acknowledgements. We thank D. van As for initial discussions on this topic, D. Pollard for comments, and M. Morlighem and X. Fettweis for providing accessible and documented data. K. D. Mankoff was funded by NASA Headquarters under the NASA Earth and Space Science Fellowship Program (Grant NNX10AN83H) and the Postdoctoral Scholar Program at the Woods Hole Oceanographic Institution, with funding provided by the Ocean and Climate Change Institute. S. Tulaczyk was funded by NASA grant NNX11AH61G. Anonymous referees contributed greatly to the focus and scope of the manuscript.

References

Alley, R. B., Lawson, D. E., Evenson, E. B., Strasser, J. C., and Larson, G. J.: Glaciohydraulic supercooling: a freeze-on mechanism to create stratified, debris-rich basal ice: II. Theory, Journal of Glaciology, 44, 563–569, 1998.

Andrews, L. C., Catania, G. A., Hoffman, M. J., Gulley, J. D., Lüthi, M. P., Ryser, C., Hawley, R. L., and Neumann, T. A.: Direct observations of evolving subglacial drainage beneath the Greenland Ice Sheet, Nature, 514, 80–83, doi:10.1038/nature13796, 2014.

Arnold, N. S., Banwell, A. F., and Willis, I. C.: High-resolution modelling of the seasonal evolution of surface water storage on the Greenland Ice Sheet, The Cryosphere, 8, 1149–1160, doi:10.5194/tc-8-1149-2014, 2014.

Banwell, A. F., Willis, I. C., and Arnold, N. S.: Modelling subglacial water routing at Paakitsoq, W Greenland, Journal of Geophysical Research: Earth Surface, pp. 1282–1295, doi:10.1002/jgrf.20093, 2013.

Bartholomew, I. D., Nienow, P. W., Sole, A. J., Mair, D. W. F., Cowton, T. R., King, M. A., and Palmer, S.: Seasonal variations in Greenland Ice Sheet motion: Inland extent and behaviour at higher elevations, Earth and Planetary Science Letters, 307, 271 – 278, doi:10.1016/j.epsl.2011.04.014, 2011.

Bell, R. E., Tinto, K. J., Das, I., Wolovick, M., Chu, W., Creyts, T. T., Frearson, N., Abdi, A., and Paden, J. D.: Deformation, warming and softening of Greenland's ice by refreezing meltwater, Nature Geoscience, 7, 497–502, doi:10.1038/NGEO2179, 2014.

Björnsson, H.: Understanding jokulhlaups: from tale to theory, Journal of Glaciology, 56, 1002–1010, 2010.

Bogen, J. and Bønsnes, T. E.: Erosion and sediment transport in High Arctic rivers, Svalbard, Polar Research, 22, 175–189, doi:10.1111/j.1751-8369.2003.tb00106.x, 2003.

Bougamont, M., Christoffersen, P., Hubbard, A. L., Fitzpatrick, A. A., Doyle, S. H., and Carter, S. P.: Sensitive response of the Greenland Ice Sheet to surface melt drainage over a soft bed, Nature Communications, 5, 5052, doi:10.1038/ncomms6052, 2014.

Brinkerhoff, D. J., Meierbachtol, T. W., Johnson, J. V., and Harper, J. T.: Sensitivity of the frozen/melted basal boundary to perturbations of basal traction and geothermal heat flux: Isunnguata Sermia, western Greenland, Annals of Glaciology, 52, 43 – 50, doi:10.3189/172756411799096330, 2011.

Catania, G. A. and Neumann, T. A.: Persistent englacial drainage features in the Greenland Ice Sheet, Geophysical Research Letters, 37, doi:10.1029/2009GL041108, 2010.

Chikita, K. A., Kaminaga, R., Kudo, I., Wada, T., and Kim, Y.: Parameters determining water temperature of a proglacial stream: The Phelan Creek and the Gulkana Glacier, Alaska, River Research and Applications, 26, 995–1004, 2010.

Clarke, G. K. C.: Hydraulics of subglacial outburst floods: new insights from the Spring-Hutter formulation, Journal of Glaciology, 49, 299–313, 2003.

Cowton, T., Nienow, P., Bartholomew, I. D., Sole, A., and Mair, D. W. F.: Rapid erosion beneath the Greenland ice sheet, Geology, 40, 343–346, doi:10.1130/G32687.1, 2012.

Cuffey, K. M. and Paterson, W. S. B.: The physics of glaciers, Academic Press, fourth edn., 2010.

Dow, C. F., Kulessa, B., Rutt, I. C., Doyle, S. H., and Hubbard, A.: Upper bounds on subglacial channel development for interior regions of the Greenland ice sheet, Journal of Glaciology, 60, 1044–1052, doi:10.3189/2014JoG14J093, 2014.

Engelhardt, H. and Kamb, B.: Basal hydraulic system of a West Antarctic ice stream: constraints from borehole observations, Journal of Glaciology, 43, 207–230, 1997.

Evans, E. C., McGregor, G. R., and Petts, G. E.: River energy budgets with special reference to river bed processes, Hydrological Processes, 12, 575–595, 1998.

The Cryosphere Discuss., doi:10.5194/tc-2016-113, 2016
Manuscript under review for journal The Cryosphere
Published: 3 June 2016

Fahnestock, M., Abdalati, W., Joughin, I. R., Brozena, J., and Gogineni, P. S.: High geothermal heat flow, basal melt, and the origin of rapid ice flow in central Greenland, Science, 294, 2338–2342, doi:10.1126/science.1065370, 2001.

Fettweis, X., Franco, B., Tedesco, M., van Angelen, J. H., Lenaerts, J. T. M., van den Broeke, M. R., and Gallée, H.: Estimating Greenland ice sheet surface mass balance contribution to future sea level rise using the regional atmospheric climate model MAR, The Cryosphere, 7, 469 – 489, doi:10.5194/tc-7-469-2013, 2013.

Fountain, A. G.: Borehole water-level variations and implications for the subglacial hydraulics of South Cascade Glacier, Washington State, USA, Journal of Glaciology, 40, 1994.

Fountain, A. G. and Walder, J. S.: Water flow through temperate glaciers, Reviews of Geophysics, 36, 299–328, 1998.

Gulley, J. D.: Structural control of englacial conduits in the temperate Matanuska Glacier, Alaska, USA, Journal of Glaciology, 55, 681–690, 2009.

Gulley, J. D., Spellman, P. D., Covington, M. D., Martin, J. B., Benn, D. I., and Catania, G. A.: Large values of hydraulic roughness in subglacial conduits during conduit enlargement: Implications for modeling conduit evolution, Earth Surface Processes and Landforms, 39, 296–310, doi:10.1002/esp.3447, 2014.

Hanna, E., Huybrechts, P., Steffen, K., Cappelen, J., Huff, R., Shuman, C., Irvine-Fynn, T., Wise, S., and Griffiths, M.: Increased runoff from melt from the Greenland Ice Sheet: a response to global warming, Journal of Climate, 21, 331–341, doi:10.1175/2007JCLI1964.1, 2008.

Herman, F., Beyssac, O., Brughelli, M., Lane, S. N., Leprince, S., Adatte, T., Lin, J. Y. Y., Avouac, J.-P., and Cox, S. C.: Erosion by an Alpine glacier, Science, 350, 193–195, doi:10.1126/science.aab2386, 2015.

Hewitt, I. J.: Modelling distributed and channelized subglacial drainage: the spacing of channels, Journal of Glaciology, 57, 2011.

Hewitt, I. J.: Seasonal Changes in Ice Sheet Motion due to Melt Water Lubrication, Earth and Planetary Science Letters, 371–372, 16–25, doi:10.1016/j.epsl.2013.04.022, 2013.

Hock, R. and Hooke, R. L.: Evolution of the internal drainage system in the lower part of the ablation area of Storglaciären, Sweden, Geological Society of America Bulletin, 105, 537–546, doi:10.1130/0016-7606(1993)105<0537:EOTIDS>2.3.CO;2, 1993.

Hooke, R. L.: Principles of Glacier Mechanics, Cambridge University Press, 2nd edn., doi:10.1017/CBO9780511614231, 2005.

Iken, A. and Bindschadler, R. A.: Combined measurements of subglacial water pressure and surface velocity of Findelengletscher, Switzerland: conclusions about drainage system and sliding mechanism, Journal of Glaciology, 32, 101–119, 1986.

Isenko, E., Naruse, R., and Mavlyudov, B.: Water temperature in englacial and supraglacial channels: Change along the flow and contribution to ice melting on the channel wall, Cold Regions Science and Technology, 42, 53–62, doi:10.1016/j.coldregions.2004.12.003, 2005.

Kamb, B.: Sliding motion of glaciers: theory and observation, Reviews of Geophysics, 8, 673–728, 1970.

Kamb, B.: Glacier surge mechanism based on linked cavity configuration of the basal water conduit system, Journal of Geophysical Research, 92, 9083–9100, 1987.

Koppes, M. N. and Marchant, D. R.: The relative efficacy of fluvial and glacial erosion over modern to orogenic timescales, Nature Geoscience, 2, 644–647, doi:10.1038/NGEO616, 2009.

Lewis, S. M. and Smith, L. C.: Hydrologic drainage of the Greenland ice sheet, Hydrological Processes, 23, 2004–2011, doi:10.1002/hyp.7343, 2009.

Liestøl, O.: Glacier Dammed Lakes in Norway, vol. 81, Fabritius & Sønners Forlag, 1956.

Lüthi, M. P., Ryser, C., Andrews, L. C., Catania, G. A., Funk, M., Hawley, R. L., Hoffman, M. J., and Neumann, T. A.: Heat sources within the Greenland Ice Sheet: dissipation, temperate paleo-firn and cryo-hydrologic warming, The Cryosphere, 9, 245–253, doi:10.5194/tc-9-245-2015, 2015.

Mathews, W. H.: Record of two jökullhlaups, in: From the Symposium on the hydrology of glaciers. International Association of Scientific Hydrology, vol. 95, pp. 99–110, 1973.

Mayaud, J. R., Banwell, A. F., Arnold, N. S., and Willis, I. C.: Modeling the response of subglacial drainage at Paakitsoq, West Greenland, to 21st century climate change, Journal of Geophysical Research: Earth Surface, 119, 2619–2634, doi:10.1002/2014JF003271, 2014.

Meierbachtol, T. W., Harper, J., and Humphrey, N.: Basal Drainage System Response to Increasing Surface Melt on the Greenland Ice Sheet, Science, 341, 777–779, doi:10.1126/science.1235905, 2013.

Meierbachtol, T. W., Harper, J. T., Johnson, J. V., Humphrey, N. F., and Brinkerhoff, D. J.: Thermal boundary conditions on Western Greenland: observational constraints and impacts on the modeled thermo-mechanical state, Journal of Geophysical Research: Earth Surface, 120, 623–636, doi:10.1002/2014JF003375, 2015.

Morlighem, M., Rignot, E. J., Mouginot, J., Seroussi, H., and Larour, E.: Deeply incised submarine glacial valleys beneath the Greenland ice sheet, Nature Geoscience, 7, 418–422, doi:10.1038/NGEO2167, 2014.

Morlighem, M., Rignot, E. J., Mouginot, J., and Seroussi, H.: IceBridge BedMachine Greenland, Version 2, doi:10.5067/AD7B0HQNSJ29, nASA DAAC at the National Snow and Ice Data Center, 2015.

Moss, R. H., Edmonds, J. A., Hibbard, K. A., Manning, M. R., Rose, S. K., van Vuuren, D. P., Carter, T. R., Emori, S., Kainuma, M., Kram, T., Meehl, G. A., Mitchell, J. F. B., Nakicenovic, N., Riahi, K., Smith, S. J., Stouffer, R. J., Thomson, A. M., Weyant, J. P., and Wilbanks, T. J.: The next generation of scenarios for climate change research and assessment, Nature, 463, 747–756, doi:10.1038/nature08823, 2010.

Neteler, M., Bowman, M., Landa, M., and Metz, M.: GRASS GIS: a multi-purpose Open Source GIS, Environmental Modelling & Software, 31, 124–130, doi:10.1016/j.envsoft.2011.11.014, 2012.

Nye, J. F.: Water flow in glaciers: jökulhlaups, tunnels and veins, Journal of Glaciology, 17, 181 – 207, 1976.

Parizek, B. R. and Alley, R. B.: Implications of increased Greenland surface melt under global-warming scenarios: ice-sheet simulations, Quaternary Science Reviews, 23, 1013–1027, doi:10.1016/j.quascirev.2003.12.024, 2004.

Phillips, T., Rajaram, H., Colgan, W., Steffen, K., and Abdalati, W.: Evaluation of cryo-hydrologic warming as an explanation for increased ice velocities in the wet snow zone, Sermeq Avannarleq, West Greenland, Journal of Geophysical Research: Earth Surface, 118, 1241–1256, doi:10.1002/jgrf.20079, 2013.

Poinar, K., Joughin, I., Das, S. B., Behn, M. D., Lenaerts, J. T. M., and Broeke, M. R.: Limits to future expansion of surface-melt-enhanced ice flow into the interior of western Greenland, Geophysical Research Letters, 42, 1800–1807, doi:10.1002/2015GL063192, 2015.

Pollard, D. and DeConto, R. M.: Description of a hybrid ice sheet-shelf model, and application to Antarctica, Geoscientific Model Development, 5, 1273–1295, doi:10.5194/gmd-5-1273-2012, 2012.

Rist, S.: Jökulsá á Fjöllum Brádabirgdayfirlit, 1954.

Rogozhina, I., Hagedoorn, J. M., Martinec, Z., Fleming, K., Soucek, O., Greve, R., and Thomas, M.: Effects of uncertainties in the geothermal heat flux distribution on the Greenland Ice Sheet: An assessment of existing heat flow models, Journal of Geophysical Research: Earth Surface, 117, doi:10.1029/2011JF002098, 2012.

Röthlisberger, H.: Water pressure in intra- and subglacial channels, Journal of Glaciology, 11, 177 – 203, 1972.

Schoof, C. G.: Ice-sheet acceleration driven by melt supply variability, Nature, 468, 803–806, doi:10.1038/nature09618, 2010.

Schulte, E. and Davison, D.: Active documents with Org-mode, Computing in Science & Engineering, 13, 66–73, 2011.

Schulte, E., Davison, D., Dye, T., and Dominik, C.: A multi-language computing environment for literate programming and reproducible research, Journal of Statistical Software, 46, 1–24, 2012.

Shannon, S. R., Payne, A. J., Bartholomew, I. D., van den Broeke, M. R., Edwards, T. L., Fettweis, X., Gagliardini, O., Gillet-Chaulet, F., Goelzer, H., Hoffman, M. J., Huybrechts, P., Mair, D. W. F., Nienow, P. W., Perego, M., Price, S. F., Smeets, C. J. P. P., Sole, A. J., van de Wal, R. S. W., and Zwinger, T.: Enhanced basal lubrication and the contribution of the Greenland ice sheet to future sea-level rise, Proceedings of the National Academy of Sciences, 110, 14 156–14 161, doi:10.1073/pnas.1212647110, 2013.

Shapiro, N. M. and Ritzwoller, M. H.: Inferring Surface Heat Flux Distributions Guided by a Global Seismic Model: Particular Application to Antarctica, Earth and Planetary Science Letters, 223, 213–224, doi:10.1016/j.epsl.2004.04.011, 2004.

Shreve, R. L.: Movement of water in glaciers, Journal of Glaciology, 11, 205–214, 1972.

Sundal, A. V., Shepherd, A., Nienow, P. W., Hanna, E., Palmer, S., and Huybrechts, P.: Melt-induced speed-up of Greenland ice sheet offset by efficient subglacial drainage, Nature, 469, 521–524, doi:10.1038/nature09740, 2011.

Tedstone, A. J., Nienow, P. W., Gourmelen, N., Dehecq, A., Goldberg, D., and Hanna, E.: Decadal slowdown of a land-terminating sector of the Greenland Ice Sheet despite warming, Nature, 526, 692–695, doi:10.1038/nature15722, 2015.

Tsai, V. C. and Rice, J. R.: A model for turbulent hydraulic fracture and application to crack propagation at glacier beds, Journal of Geophysical Research: Earth Surface, 115, doi:10.1029/2009JF001474, 2010.

Tulaczyk, S. M., Kamb, W. B., and Engelhardt, H. F.: Basal mechanics of Ice Stream B, West Antarctica 1. Till mechanics, Journal of Geophysical Research, 105, 463 – 481, 2000.

Walter, J. I., Box, J. E., Tulaczyk, S. M., Brodsky, E. E., Howat, I. M., Ahn, Y., and Brown, A.: Oceanic mechanical forcings of the dynamics of a marine-terminating Greenland glacier by ice mélange removal and ocean tides, Annals of Glaciology, 53, 181 – 192, doi:10.3189/2012AoG60A083, 2012.

Weertman, J.: The Theory of Glacier Sliding, Journal of Glaciology, 5, 287–303, 1964.

Yang, K. and Smith, L. C.: Supraglacial Streams on the Greenland Ice Sheet Delineated From Combined Spectral–Shape Information in High-Resolution Satellite Imagery, IEEE Geoscience and Remote Sensing Letters, 10, 801 – 805, doi:10.1109/LGRS.2012.2224316, 2013.

Yang, K., Smith, L. C., Chu, V. W., Gleason, C. J., and Li, M.: A Caution on the Use of Surface Digital Elevation Models to Simulate Supraglacial Hydrology of the Greenland IIce Sheet, IEEE Journal of Selected Topics in Applied Earth Observations and Remote Sensing, pp. 1–13, doi:10.1109/JSTARS.2015.2483483, 2015.

Zwally, H. J., Abdalati, W., Herring, T., Larson, K., Saba, J. L., and Steffen, K.: Surface melt-induced acceleration of Greenland ice-sheet flow, Science, 297, 218–222, 2002.

The Cryosphere Discuss., doi:10.5194/tc-2016-113, 2016
Manuscript under review for journal The Cryosphere
Published: 3 June 2016

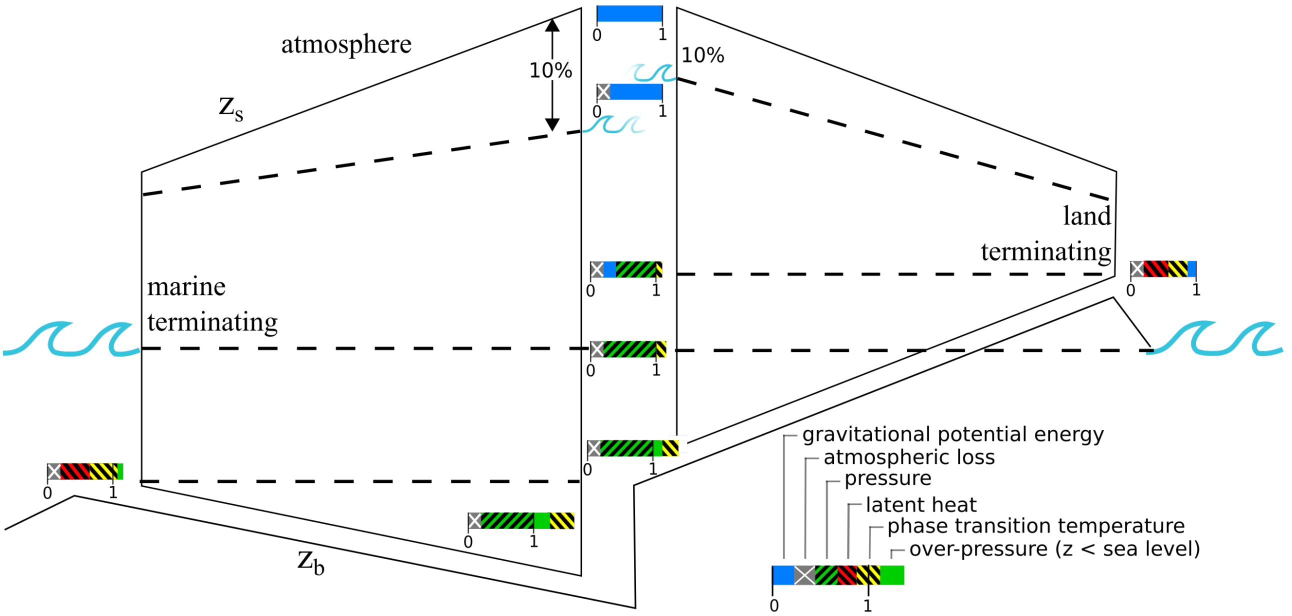

Figure 1. Schematic of a water-filled moulin and a land- and marine-terminating glacier. Bar graphs show form and amount of energy relative to initial gravitational potential energy and sea level, at different locations throughout the system. On the bar graphs, 1 represents an energy state equivalent to a 0 °C parcel with no velocity at some elevation, z_s, equal to the ice sheet surface. 0 represents an energy state equivalent to that same parcel of liquid water at 0 °C with no velocity at sea level.

The Cryosphere Discuss., doi:10.5194/tc-2016-113, 2016
Manuscript under review for journal The Cryosphere
Published: 3 June 2016

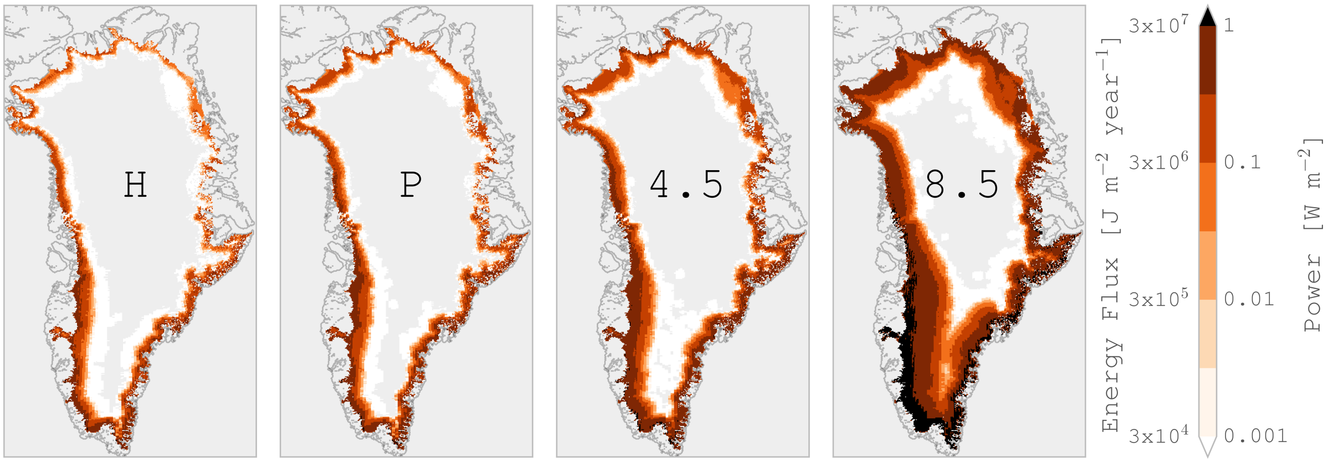

Figure 2. Gravitational potential energy from surface runoff. Labels represent (H)istorical mean runoff from 1900 – 1999, (P)resent mean runoff from 2010 – 2019, (4.5) years 2090 – 2099 under IPCC AR5 RCP4.5, and (8.5) same as (4.5) but under scenario RCP8.5. Gray contour marks 0 m elevation.

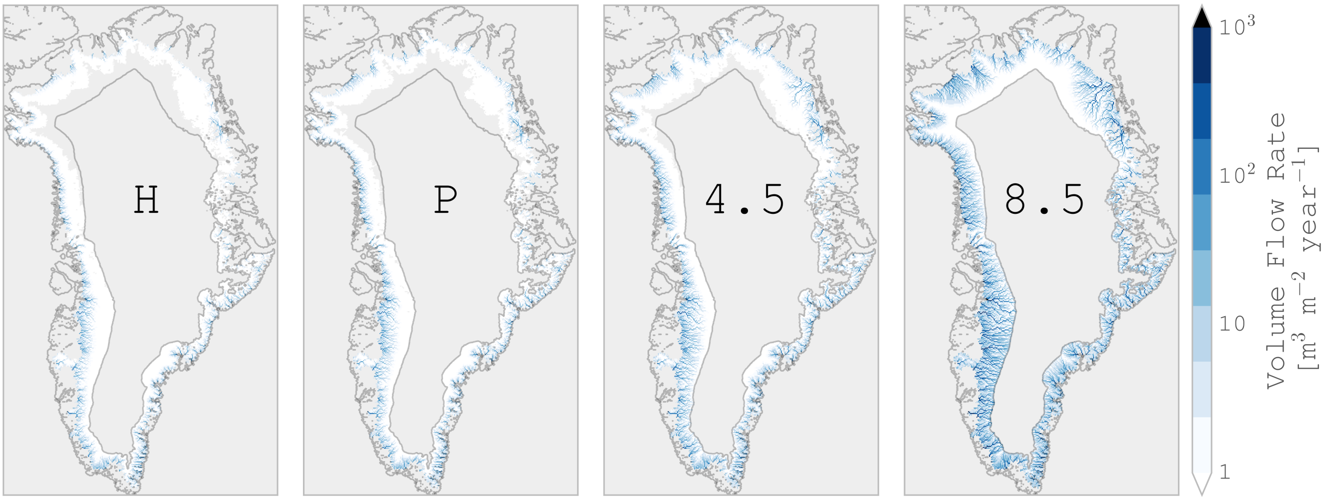

Figure 3. Accumulation of subglacial water flowing through each grid cell. Results are presented on a 5x5 km grid. Labels same as Fig. 2. Gray contours mark 0 and 2000 m elevation.

The Cryosphere Discuss., doi:10.5194/tc-2016-113, 2016
Manuscript under review for journal The Cryosphere
Published: 3 June 2016

The Cryosphere
Discussions
Open Access

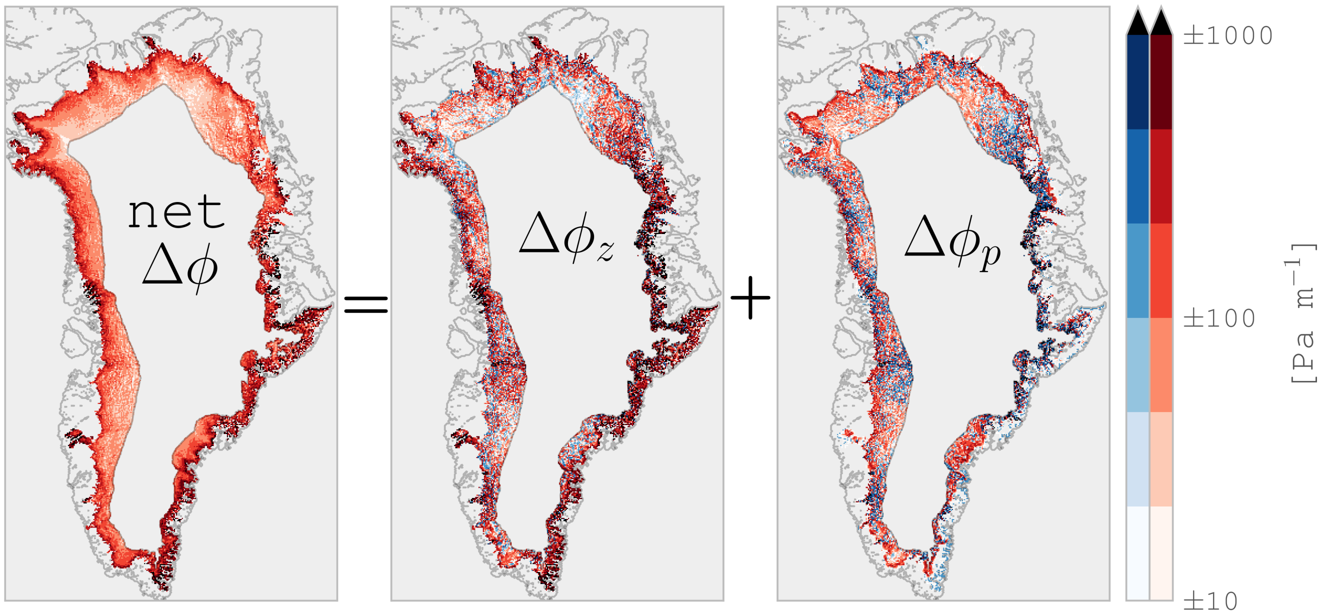

Figure 4. Net hydropotential change between each cell and its downstream neighbor ($\Delta\phi$, and the decomposition of net hydropotential change to elevation-driven hydropotential ($\Delta\phi_z$) and pressure-driven hydropotential ($\Delta\phi_p$). Red is positive and blue is negative. Negative $\Delta\phi_z$ implies flow uphill driven by a pressure gradient, and positive $\Delta\phi_p$ implies flow driven by thinning ice. Large differences in released heat (~66%) are due to flow under thinning or thickening ice.

The Cryosphere Discuss., doi:10.5194/tc-2016-113, 2016
Manuscript under review for journal The Cryosphere
Published: 3 June 2016

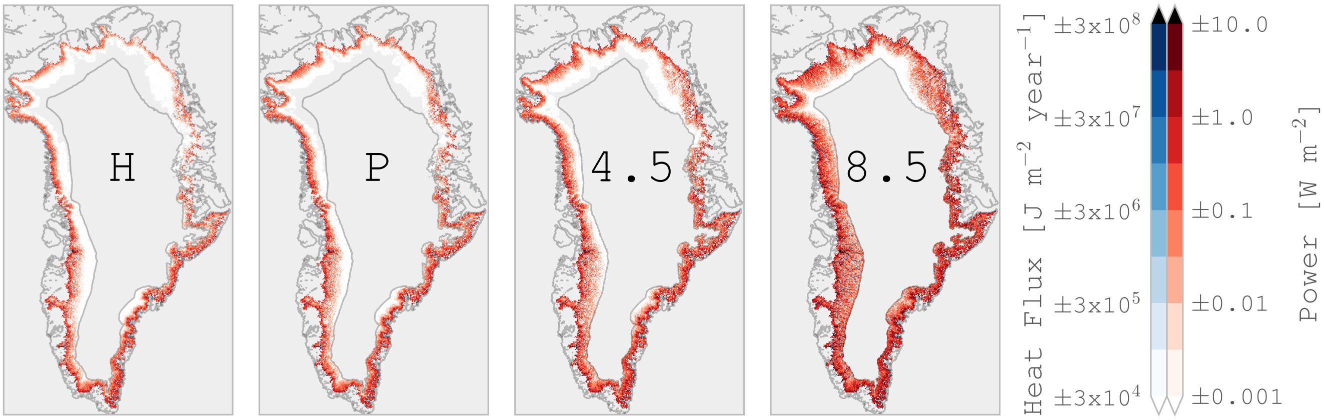

Figure 5. Heat released at the bed. Labels same as Fig. 2. Colorbars represent heating (red) and cooling (blue), and numbers are valid for both colorbars (i.e. 1 W m^{-2} equals 3x10^7 J m^2 year^{-1}, and each of those values are positive on the red colorbar and negative on the blue colorbar). Gray contours mark 0 and 2000 m elevation.

The Cryosphere Discuss., doi:10.5194/tc-2016-113, 2016
Manuscript under review for journal The Cryosphere
Published: 3 June 2016

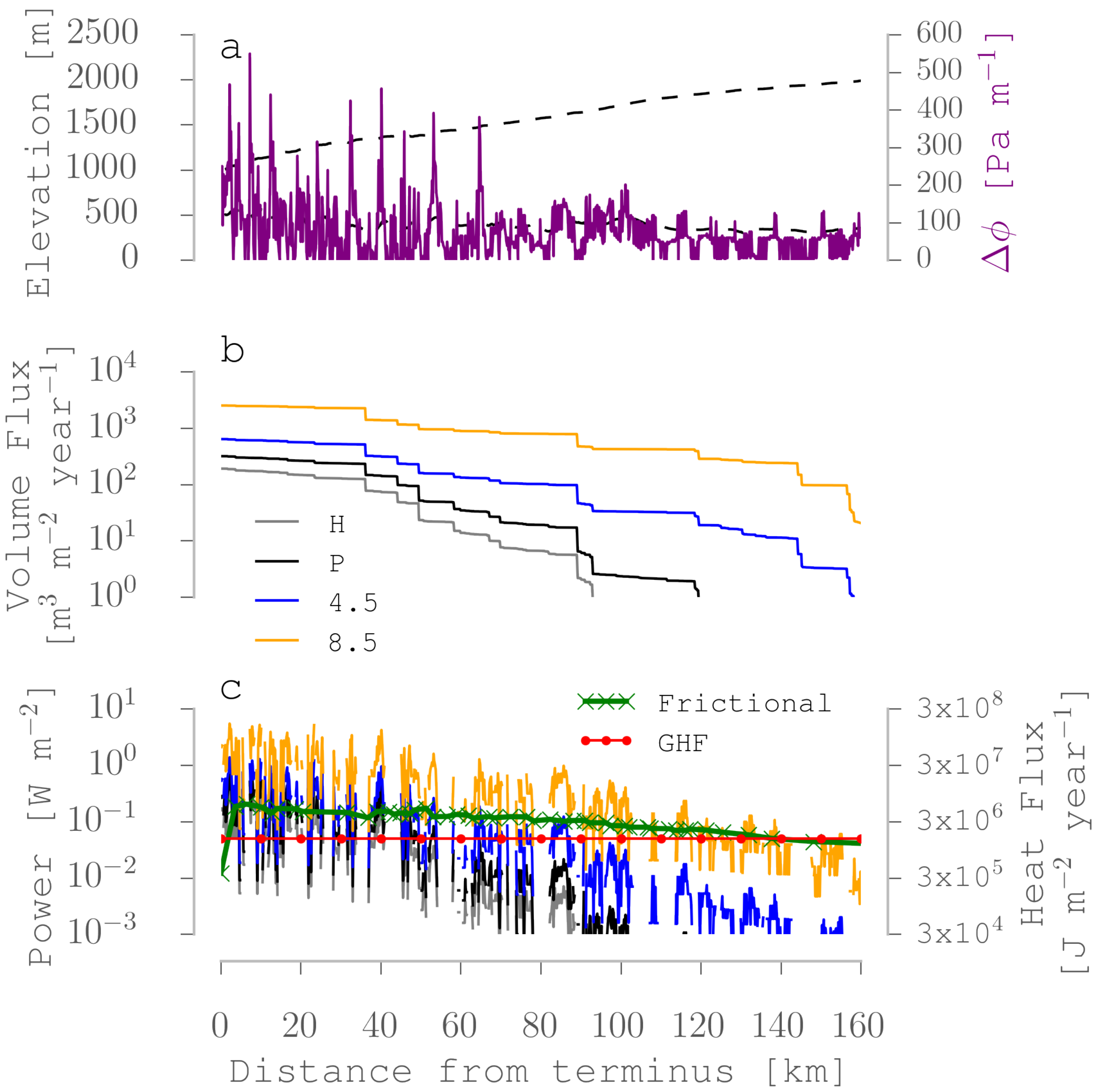

Figure 6. Detail along a flowline on Russell glacier. a) surface and bed elevation (left axis) and change in ϕ (right axis), b) flow rate, and c) power, frictional heating, and geothermal heat flux. Legend labels H, P, 4.5, and 8.5 same as Fig. 2. Frictional heating from Brinkerhoff et al. (2011), and geothermal heat flux (GHF) from Shapiro and Ritzwoller (2004).

The Cryosphere Discuss., doi:10.5194/tc-2016-113, 2016
Manuscript under review for journal The Cryosphere
Published: 3 June 2016

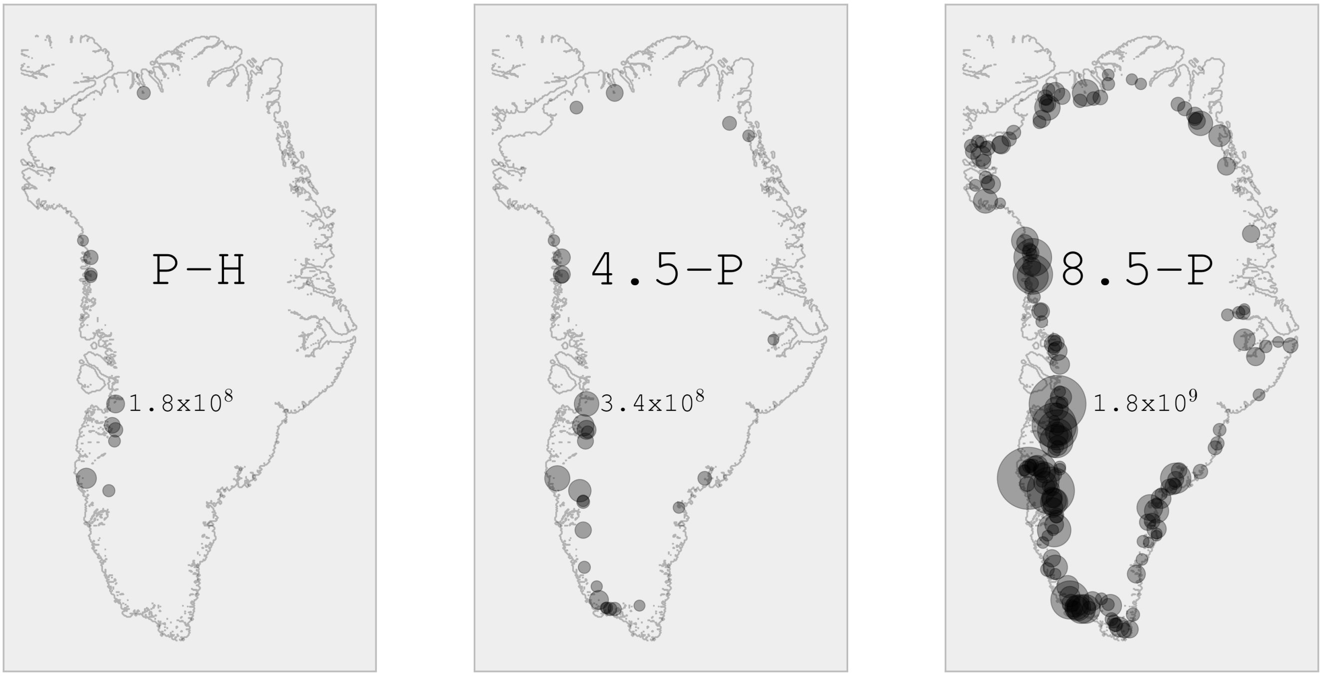

Figure 7. Change in cumulative upstream heat released at the bed. Label P-H represents increase from historical to present, 4.5-P difference between present and 2090s under RCP 4.5, and similarly for 8.5-P. Symbols show amount of heat released between terminus and upstream source for each flowline. Numbers (units are Joule) are a legend for the changing size of one symbol. Increases of less than 2×10^8 J are not shown.

The Cryosphere Discuss., doi:10.5194/tc-2016-113, 2016
Manuscript under review for journal The Cryosphere
Published: 3 June 2016

Table 1. Properties of Greenland runoff and viscous heat dissipation. (H)istorical period covers 1900 – 1999, (P)resent spans 2010 – 2019, and the RCP(4.5) and (8.5) periods span 2090 – 2099. Runoff volume and area from MAR (Fettweis et al., 2013), elevation from MAR combined with IceBridge BedMachine Greenland, Version 2 (Morlighem et al., 2015, 2014). Geothermal heat flux from Shapiro and Ritzwoller (2004) calculated only under runoff area.

Property	Units	H	P	4.5	8.5
Runoff volume	km^3 $year^{-1}$	254	345	526	1288
Runoff area	10^6 km^2	0.68	0.68	0.84	1.23
Runoff mean elevation $\bar{z}_s$	m	1293	1296	1344	1398
Runoff weighted mean elevation $\bar{z}_s$	m	837	863	955	1109
Maximum discharge per 5x5 km grid	km^3 $year^{-1}$	5	7	10	32
Potential energy	10^{18} J $year^{-1}$	2.1	2.9	4.9	14.3
Viscous heat dissipation	10^{18} J $year^{-1}$	1.4	1.9	3.2	9.0
Geothermal heat flux	10^{18} J $year^{-1}$	1.1	1.1	1.3	1.4